JOURNAL OF Materials CHEMISTRY

Dicalcium nitride, Ca_2N—a 2D "excess electron" compound; synthetic routes and crystal chemistry†

Duncan H. Gregory,*[a] Amy Bowman,[a] Charles F. Baker[a] and David P. Weston[b]

[a]*School of Chemistry, University of Nottingham, Nottingham, UK NG7 2RD*
[b]*School of Mechanical, Materials, Manufacturing Engineering and Management, University of Nottingham, Nottingham, UK NG7 2RD. E-mail: Duncan.Gregory@Nottingham.ac.uk*

Received 9th March 2000, Accepted 3rd May 2000
Published on the Web 21st June 2000

The subnitride Ca_2N has been prepared *via* several synthetic routes described for the first time, including reduction of Ca_3N_2 and reaction of Ca metal dissolved in liquid sodium with nitrogen gas. Products have been characterised by powder X-ray and powder neutron diffraction. Crystallite morphology and compound stoichiometry have been examined by SEM/EDAX. Ca_2N crystallises with a hexagonal layered structure in space group $R\bar{3}m$ ($a=3.62872(3)$ Å, $c=19.0921(4)$ Å, $V=217.72(1)$ Å^3, $Z=3$, $c/a=5.26$). $[NCa_2]^+$ layers composed of compressed, edge-sharing NCa_6 octahedra stack along the *c*-axis and are separated by large "van der Waals" gaps. The material is metallic and paramagnetic at room temperature. The *c*-parameter, $[NCa_2]^+$ layer thickness and interlayer gap are larger than previously reported and there is no evidence of hydride or other anion intercalation between layers.

Introduction

The binary nitrides of the alkali and alkaline earth metals have aroused a great deal of curiosity over many decades. Of the alkali metals, only lithium forms a stable nitride, Li_3N, which itself has a unique structure.[1] The alkaline earth metals form compositions strongly correlated to their electropositivities; Be_3N_2 and Mg_3N_2 might be considered "classically ionic". On the basis of reliable structural data, the heavier Group 2 metals Sr and Ba form exclusively subnitrides (*e.g.* Sr_2N, Ba_3N)[2,3] in which metallic bonding appears to become a crucial factor. Calcium, however, occupies a unique position, forming the ionic nitride, Ca_3N_2[4] and also the subnitride, Ca_2N.[5,6] Other binary nitride compounds of the alkaline earth metals have been reported but the veracity of the stoichiometry and crystal chemistry of these phases is open to question (a pertinent example of this is the recent identification of "$Ca_{11}N_8$" as the nitride cyanamide, $Ca_{11}N_6(CN_2)_2$).[7]

Recent studies of the strontium–nitrogen and barium–nitrogen systems have clarified earlier investigations of the crystal chemistry of the heavier Group 2 subnitrides and provided evidence of further phases.[2,3,8] The binary compounds have been shown to be part of a rich vein of cluster chemistry in Group 1– and Group 2–nitrogen systems.[9] The Ba–Na–N system has already produced an exotic selection of "void metal" subnitrides. The structures of $NaBa_3N$ and Na_5Ba_3N, for example, contain 1D chains of Ba–N ionic, insulating, cores ("antiwires") surrounded by a Na metallic, conducting matrix.[10]

Recent work has indicated that a similarly diverse subnitride chemistry may exist for calcium with, for example, silver ($Ag_{16}Ca_6N$, $Ag_8Ca_{19}N_7$)[11,12] and gold ($AuCa_2N$, $AuCa_3N$).[13,14] These compounds show that 0, 2 and 3D structure types are possible in Ca–(M)–N systems. Surprisingly however, despite its fundamental nature as a binary compound, calcium subnitride, Ca_2N, remains incredibly ill defined. Originally, the nitride was reported to be obtainable by the reaction of calcium metal with α-Ca_3N_2 in a sealed system at 1100 °C.[5] The crystal structure of Ca_2N was reported in 1968, although no absorption correction was applied and the refinement showed some inconsistencies owing to the acknowledged poor quality of the crystal.[6b] No information as to how the studied crystal was prepared was reported and, indeed, very little detail regarding methods of synthesis for Ca_2N has yet been presented in the open literature. A regular point of debate in subnitride chemistry has been the existence or otherwise of intercalated light anions, such as hydride, within the 1D or 2D structures and whether, therefore, these compounds can be termed "nitride electrides". We report here the result of our systematic investigations into an array of synthetic routes to dicalcium nitride and our subsequent characterisation of the bulk products so obtained.

Experimental

Synthesis of Ca_2N by reduction of Ca_3N_2 under argon

A phase approximating to the structural description of Ca_2N was first detected in powder X-ray diffraction (PXD) patterns as a by-product of reactions of calcium nitride, Ca_3N_2, with transition metal powders under argon in sealed-system, high temperature, solid state reactions. Initially, we aimed to isolate this product by performing "control" reactions under the same conditions (*i.e. without* the presence of transition metal powders).

The starting material, Ca_3N_2, for these and subsequent syntheses was prepared by the reaction of the molten alkaline earth metal–sodium alloy with dried nitrogen at 600 °C using a method detailed fully elsewhere.[15] Molten alkali and alkaline earth metals are highly reactive to air and water and these were handled in inert atmospheres at all times. Excess sodium was removed by heating under vacuum at 400 °C for 24 h. Liquid sodium is unreactive towards nitrogen and serves as an inert solvent for the alkaline earth metals. This method produces calcium nitride containing negligible amounts of the alkaline earth oxide. The reaction yielded polycrystalline samples of dark red Ca_3N_2. The identity of α-Ca_3N_2[16] was confirmed by PXD with reference to the ICDD (JCPDS) database (card number 4-854).

The subnitride Ca_2N was synthesised by reduction of Ca_3N_2

†Electronic supplementary information (ESI) available: XRD and POLARIS neutron diffraction refinements. See http://www.rsc.org/suppdata/jm/b0/b001911i/

DOI: 10.1039/b001911i

under purified argon in sealed systems at high temperature. All manipulations were carried out in a purified argon filled evacuable glove box (*ca.* 5 ppm H_2O, <5 ppm O_2). Pellets of ground Ca_3N_2 powder were wrapped in cleaned molybdenum foil tubes and placed within stainless steel crucibles which were subsequently welded closed under purified argon. Stainless steel crucibles were fired in a tube furnace at temperatures between *ca.* 1000–1125 °C for 5 days under flowing argon to prevent oxidation of the steel and then cooled at 20 °C h^{-1} to room temperature, again under flowing argon. The outer surfaces of the cooled crucibles were mechanically cleaned to remove any oxidised steel. The cleaned crucibles were then cut open in a nitrogen-filled glove box. The reactions yielded microcrystalline powders of a platey habit and varying in colour, depending on reaction temperature, from purple ($\leqslant$1000 °C) through to black ($\approx$1100 °C). The higher temperature products were extremely air-sensitive and changed colour from black to white after only a few seconds of exposure. The powders also reacted violently and exothermically (almost explosively) with water evolving ammonia.

Synthesis of Ca_2N by reduction of Ca_3N_2 under vacuum

More facile reductions at lower temperatures were achieved by heating ground Ca_3N_2 powder under a dynamic vacuum ($\approx 10^{-6}$–10^{-7} mbar). All manipulations were carried out in a purified-nitrogen filled recirculating glove box (*ca.* 5 ppm H_2O, <1 ppm O_2). Powdered or pelleted samples of the binary nitride were wrapped in cleaned molybdenum foil and sealed in a stainless steel, alumina or silica vessel. The vessel was connected to a vacuum line and evacuated using Edwards rotary and diffusion pumps. Samples were heated to temperatures of 900–1000 °C for 2–4 days and cooled to room temperature. The reactions yielded dark green/black, moisture sensitive polycrystalline products. Samples underwent a weight loss of *ca.* 5% after reduction, consistent with formation of Ca_2N from Ca_3N_2 (eqn. (1)).

$$4Ca_3N_2 \rightarrow 6Ca_2N + N_2 \quad (1)$$

Synthesis of Ca_2N by reaction of calcium in liquid sodium with N_2 gas

Ca_2N samples could also be easily prepared at even lower temperatures *via* a more direct route starting from calcium metal. Cleaned calcium metal (Alfa, 99%) (*ca.* 8 g) was dissolved in excess liquid sodium in a stainless steel crucible at 250 °C in a purified argon-filled glove box. The Na–Ca alloy was heated to 600 °C under a constant positive nitrogen pressure (*ca.* 2 atm) within a stainless steel vessel until the gas pressure remained constant (typically *ca.* 12 h). The gas pressure was monitored throughout by means of a pressure transducer interfaced to a PC which in turn controlled addition of aliquots of N_2 as appropriate. Sodium was removed by distillation under vacuum at 480–500 °C for 24 h. Reactions yielded dark green/black polycrystalline products which reacted violently with water.

Characterisation by SEM/EDAX and analysis

Morphology of microcrystalline products was investigated by scanning electron microscopy (SEM) using a Phillips XL 30 ESEM-FEG instrument running at either 10.0 or 15.0 kV in ultra high vacuum mode. Elemental analysis was simultaneously performed by energy dispersive analysis of X-rays (EDAX), taking area and point scans of samples. The compound stoichiometry was also evaluated by weight gain to CaO by reaction under oxygen at high temperature. In the latter experiments samples, pre-weighed in a nitrogen-filled glove box, were heated in a tube furnace under flowing O_2 at *ca.* 800 °C for 6 h. The identity of the products of the oxidation reactions as CaO was confirmed by PXD.

Characterisation and structure determination by powder X-ray diffraction

PXD data were collected using a Philips XPERT θ–2θ diffractometer with CuK_α radiation. Samples were loaded in a nitrogen filled glove box and data collected using an aluminium holder with a Mylar film window and threaded removable cover with an O-ring seal, detailed more fully elsewhere.[17] Initially *ca.* 60 min scans were taken of samples over a 2θ range of 5–80° to assess purity and to determine lattice parameters. Phase purity was assessed by using the Philips IDENTIFY routine which allows access to the ICDD (JCPDS) database. Most samples contained small amounts of CaO with characteristic peaks which appeared to increase in intensity depending on scan times. We found that CaO impurity could be reduced by increasing the thickness of the Mylar film, but only by compromising reflected intensity. Remaining peaks of each pattern were indexed on a hexagonal unit cell with lattice parameters $a \approx 3.6$ Å, $c \approx 19$ Å using DICVOL91.[18,19] Lattice parameters were refined by least squares fitting of PXD data. Reflections could be assigned to space group $R\bar{3}m$ and patterns were in agreement to that calculated by POWDERCELL 2.0[20] from Keve and Skapski's model for Ca_2N from single crystal X-ray diffraction data.[6] Indexed cell parameters of samples prepared by different routes were in good agreement. Although refined *a* parameters agreed reasonably well with the previously published work, *c* parameters were consistently observed to be *ca.* 5% longer. Comparisons of the patterns with the earlier data were also complicated at this stage by the enhancement of 00*l* reflections due to preferred orientation effects. These effects were adequately reduced, for the purposes of a simple direct comparison, by collecting PXD data from samples sprinkled on to a layer of silicone grease on a glass sample slide, ensuring a more random arrangement of crystallites (Fig. 1).

Structure refinement was performed on data collected for Ca_2N samples in the range 5–130° 2θ with a step size of 0.02° 2θ over *ca.* 16 h. The quality of the final fit and agreement indices were primarily affected by two factors: first, the reaction of the nitride with air during handling and data collection to yield CaO and/or $Ca(OH)_2$ and second, 00*l* preferred orientation inherent in the Bragg–Brentano, flat plate geometry of the experiment. The first problem could be partly overcome by increasing Mylar film thickness as noted above. The second problem could be reduced by prolonged grinding and

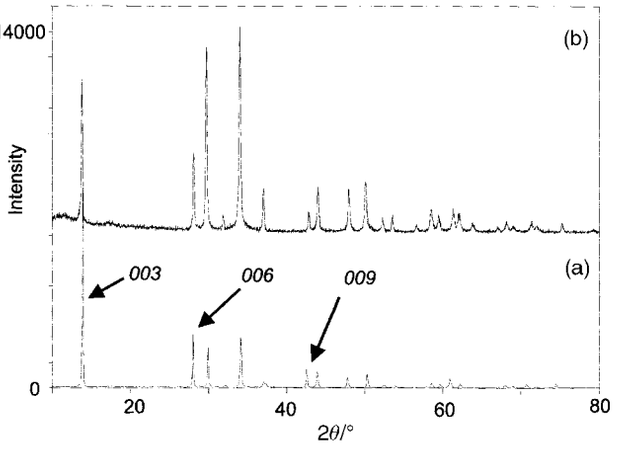

Fig. 1 Powder X-ray diffraction patterns of a Ca_2N sample synthesised *via* reduction under argon in a sealed system, (a) mounted conventionally in normal Bragg–Brentano geometry and (b) sprinkled on to a flat layer of silicone grease. The 00*l* peaks affected by preferred orientation are highlighted.

alternative loading. Use of filler materials to reduce texturing was generally unsatisfactory (silicon, for example, has overlapping reflections rendering accurate refinement near impossible). Also, whereas sprinkling powder on to silicone grease was appropriate to determine approximate relative intensities, longer scan times did not yield data of suitable quality for structure refinement. (Sample transparency, for example, is a well-known problem associated with this method.)

The structure of a vacuum reduced sample was refined by the Rietveld method[21] using two packages, PC RIETVELD PLUS[22] and FULLPROF 98,[22a,23] in an attempt to best fit the diffraction profile, particularly in terms of preferred orientation, peak shape and background handling. The final refinement using the latter software was the more satisfactory and is reported here. The Thompson–Cox–Hastings pseudo-Voigt function and a two-term March–Dollase function were used to model peak shape and preferred orientation respectively and the background was modelled as a polynomial with six refined coefficients. Initial cycles allowed for the variation of the scale factor, zeropoint and lattice parameters. As the refinement progressed atomic positions, peak width parameters and isotropic temperature factors were introduced. Anisotropic temperature factors for Ca and N were varied in final cycles but both destabilised the refinement and tended to yield negative values. CaO was simultaneously refined as an impurity phase.

Structure determination by powder neutron diffraction (PND)

Time of flight (TOF) PND data were collected for a *ca.* 1.1 g Ca_2N sample prepared in liquid sodium using the high intenisty diffractometer POLARIS at the ISIS spallation source, Rutherford Appleton Laboratory. Diffraction data were collected using the ^{3}He tube detector banks at 35 and 145° and the ZnS scintillator detector bank at 90°. This allowed data collection over a range of *d*-spacings from 0.35 to 6.7 Å. Data were collected at 298 K and 2 K for a sample contained in an electron beam welded, 6 mm diameter vanadium can with an indium gasket. The Ca_2N was pre-loaded and the can sealed in a nitrogen-filled glove box.

Rietveld refinements were performed using the general structure analysis system (GSAS).[24] Data from the three detector banks were refined simultaneously in each case following a similar strategy to the X-ray refinement above. Peak shape was modelled using TOF profile function 3 (double exponential and Gaussian convolution convoluted with pseudo-Voigt). Background was handled with function 4 (298 K) (modelling thermal diffuse scattering) or 6 (2 K) (modelling high and low Q contributions) with up to seven refined coefficients for each bank. Calcium oxide (CaO) was simultaneously refined as an impurity phase. Final cycles included profile and background parameters, scale factor and phase fractions, cell parameters, Ca(*z*), and anisotropic temperature factors for Ca and N. A small number of weak reflections not corresponding to Ca_2N, CaO or any known identifiable phase were detected. These were excluded from the refinement. Adequate fitting of some 00*l* peaks was difficult. Brese and O'Keeffe noted in their refinement of Sr_2N that the subnitride exhibited Lorentzian broadening yielding 00*l* reflections with broad bases.[2] We observed a similar phenomenon. However, it is unclear whether this is principally a strain effect or perhaps the presence of a related phase with overlapping reflections. Our attempts to identify this possible phase on the basis of these broad peaks were not successful. The broadening of these (principally 00*l*) peaks and the resulting fitting account in the main for the magnitude of the final residuals, notably for the 298 K data.

Negligible features were found in Fourier difference maps and our attempts to refine atom occupancies at positions within the interlayer gap led to no improvements in the fit, without exception. Variations where additional N was introduced yielded zero site occupancies at these positions while distributing N between the 3a (0,0,0) and, for example, 3b (0,0,1/2) sites always refined to 100% occupancy of the former position. Incorporation of H (or O, Na, for example) between layers always yielded zero or negative site occupancies. Attempts to vary the Ca site occupancy in isolation from the Ca anisotropic temperature factors produced only a 100% occupied site. Simultaneous variation of the Ca occupancy and anisotropic temperature factors led to significant correlations and destabilisation of the refinement.

Magnetic susceptibility and conductivity

Simple magnetic susceptibility and electrical conductivity experiments were performed at room temperature (293 K). Susceptibility measurements were performed using a Johnson Matthey magnetic susceptibility balance. Ground samples (*ca.* 0.1 g) were loaded into pre-weighed silica sample tubes in an argon filled glove box. Sample tubes were filled to a height of approx. 1.5 cm and sealed. After correction for the diamagnetism of the tubes, samples gave a value for mass susceptibility $\chi_g = 2.1 \times 10^{-5}$ emu g^{-1} and corresponding molar susceptibility $\chi_m = 2.0 \times 10^{-3}$ emu mol^{-1}. Conductivity measurements were performed in a nitrogen filled glove box on compressed pellets of Ca_2N samples (typical dimensions: thickness *ca.* 1.5 mm and diameter *ca.* 8 mm, measured by micrometer) using a simple four point approach. Pellets gave resistance readings of approximately 20 Ω and corresponding conductivity, $\sigma = 1.6 \times 10^{-2}\ \Omega^{-1}\ cm^{-1}$ at 293 K.

Results and discussion

Dicalcium nitride, Ca_2N, can be synthesised *via* a number of routes. In each case, the physical appearance and air stability is very similar. PXD patterns reveal products to be near identical and essentially isotypic to the model of Ca_2N originally described. Lattice parameters of these different products show an excellent level of consistency but demonstrate reproducibly larger *c*-parameters (and smaller *a*-parameters) to those previously reported (Table 1).

Ca_2N synthesised by reduction under argon was only obtained as a single phase product at temperatures above 1100 °C; below 1000 °C the only observed phase was α-Ca_3N_2 and from 1000–1100 °C both α-Ca_3N_2 and Ca_2N were obtained. The Ca–N system in liquid sodium is more complex and nitride composition hinges crucially on sodium distillation temperature. When sodium is distilled at *ca.* 350–400 °C, α-Ca_3N_2 is the only observed nitride product. At *ca.* 500 °C, single phase Ca_2N is produced with no evidence of Ca_3N_2. We are currently investigating higher and intermediate distillation temperatures. We have already observed evidence of further phases, as yet unidentified, at temperatures between 400–

Table 1 Lattice parameters (from DICVOL91)[18,19] for representative Ca_2N samples

Sample	*a*/Å	*c*/Å	*V*/Å^3	*c*/*a*
Ca_2N *via* reduction under argon	3.624(1)	19.107(8)	217.3(2)	5.3
Ca_2N *via* reduction under vacuum	3.623(1)	19.101(1)	217.1(1)	5.3
Ca_2N *via* reaction in $Na_{(l)}$	3.625(1)	19.090(9)	217.2(3)	5.3
Ca_2N from ref. 6	3.638(3)	18.780(9)	215.2(5)	5.2

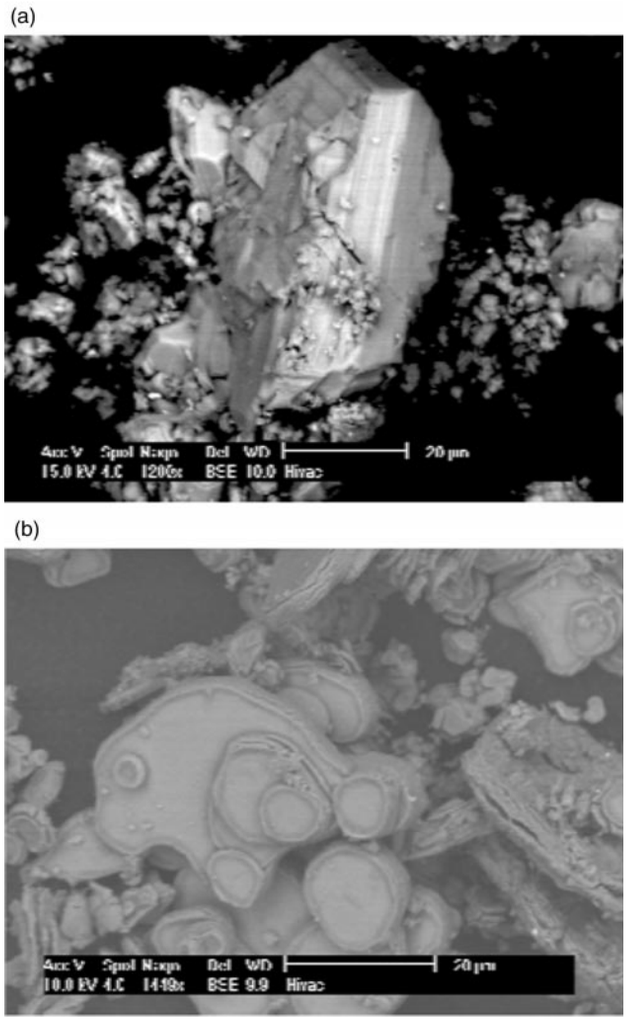

Fig. 2 Scanning electron micrographs of (a) Ca_2N reduced from Ca_3N_2 under vacuum and (b) Ca_2N prepared in liquid sodium.

500 °C. This would suggest that a range of Ca–N compositions might exist, perhaps also incorporating sodium in some way as observed previously in the Na/Ba/N system.

Analyses show a consensus for the nominal stoichiometry, Ca_2N, being correct. Ca_3N_2 undergoes a *ca.* 5% weight loss when reduced, commensurate with formation of Ca_2N as shown in eqn. (1). When heated under flowing oxygen, samples increased in weight by *ca.* 18% giving a mean stoichiometry $Ca_{1.9(1)}N$. PXD confirmed the only product of the oxidation reactions to be CaO by reference to the ICDD (JCPDS) database (card No. 4-777).

SEM reveals that morphology is dependent on the preparative route. Subnitride produced by reduction pathways without sodium contained particles of consistently ill-defined, block-like habit with sharp edges (Fig. 2a), whereas that synthesised in liquid sodium was comprised of smaller, well-defined platelets, *ca.* 6–30 μm across (Fig. 2b). Although samples were loaded into the SEM under a flow of N_2 gas, micrographs also show the rapid growth of CaO in nitride samples after seconds of air-exposure. EDAX analysis confirms this fact. Accurate nitride stoichiometry was only obtained from point scans on well-defined crystallites, relatively uncontaminated with CaO. EDAX analysis is in excellent agreement with gravimetric results with Ca : N ratios in the range 1.8 : 1 to 2.1 : 1 yielding an average value for the stoichiometry of $Ca_{2.0}N$. Importantly, EDAX also confirmed the *absence* of sodium in Ca_2N samples synthesised *via* the sodium route.

Results of the structure refinements of Ca_2N samples are presented in Table 2. The fits to the X-ray and neutron data are shown in Fig. 3. The refined atomic parameters are listed in Table 3. Quantitative analysis of the X-ray data from FULL-PROF98 yielded weight percentage values of 82% Ca_2N, 18% CaO respectively. Quantitative analysis from the neutron data shows 99% Ca_2N, 1% CaO for the 298 K data (performed first) and 97% Ca_2N, 3% CaO for the 2K data (performed *ca.* 24 h later). It is likely that the origin of the majority of the oxide impurity is from Ca_2N reacting with low ppm levels of air during handling. The higher figure observed for CaO in the X-ray data is reflective of the higher permeability of the X-ray sample holders to air over the sealed vandium cans used in PND. Noteworthy are the points that: (i) no CaO is observed as an impurity in the Ca_3N_2 starting material and (ii) no evidence of further reduction to Ca metal (which might then oxidise in part to CaO) was observed after synthesis.

The structure of Ca_2N is shown in Fig. 4. Important interatomic distances and angles are shown in Table 4. The subnitride is isostructural with Sr_2N[2] in space group $R\bar{3}m$ (*anti* $CdCl_2$-type) as previously postulated.[6] The layered structure is made up of N–Ca slabs in which N is co-ordinated octahedrally to six Ca atoms and each Ca atom is bonded to three N neighbours at a distance of 2.4426(4) Å. This value is similar to that earlier reported for Ca_2N (2.433(7) Å)[6] and α-Ca_3N_2 (2.46 Å)[4] and is close to the distance calculated from the sum of the ionic radii (also 2.46 Å).[25] Several other distances are worth highlighting at this point, notably Ca–Ca distances across and along layers (3.270(1) Å, 3.6287(6) Å) and also between layers (4.3742(2) Å). The *intra*layer Ca–Ca distances are significantly shorter than in Ca metal (3.94 Å)[26] whereas the *inter*layer distances are considerably longer. The longer *c*-parameters consistently observed in our compounds are a direct consequence of the differences in these distances from those

Table 2 Results of powder X-ray and neutron diffraction refinements of Ca_2N

Sample	Ca_2N reduced under Ar (I)	Ca_2N synthesised under Na (II)	Ca_2N synthesised under Na (II)
Radiation	X-ray (CuKα)	Neutron	Neutron
Instrument	Philips Xpert	POLARIS	POLARIS
Formula	Ca_2N	Ca_2N	Ca_2N
M	94.13	94.13	94.13
Temperature/K	298	298	2
Crystal sytem	Hexagonal	Hexagonal	Hexagonal
Space group	$R\bar{3}m$	$R\bar{3}m$	$R\bar{3}m$
a/Å	3.6235(1)	3.62872(3)	3.62194(4)
c/Å	19.1015(1)	19.0921(4)	19.0629(4)
c/*a*	5.27	5.26	5.26
V/Å^3	217.19(1)	217.72(1)	216.57(1)
Z	3	3	3
Observations, parameters	6230, 22	13554, 45	13647, 45
χ^2	3.79	7.29	5.16
R_{wp}	14.6	4.63	1.97
R_p	11.2	6.79	3.33

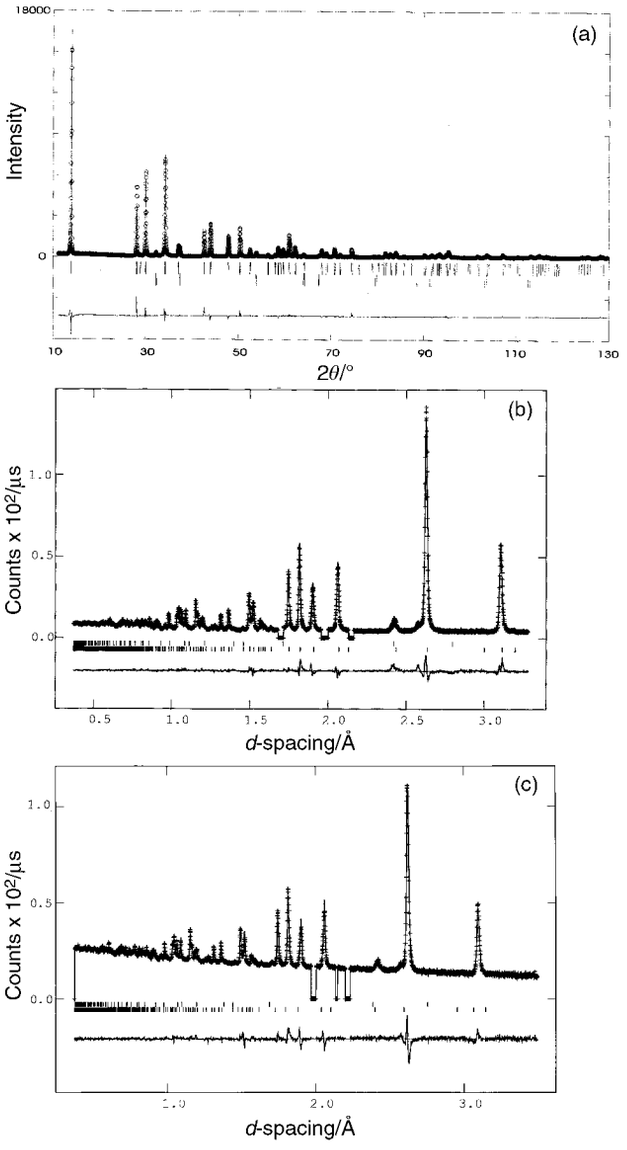

Fig. 3 Final observed (crosses or circles), calculated (solid line) and difference (below) profiles for Rietveld refinements of Ca_2N (a) synthesised under vacuum; PXD data at 298 K and (b) synthesised in liquid sodium; POLARIS PND 90° bank data at 298 K, (c) synthesised in liquid sodium; POLARIS PND 90° bank data at 2 K.

originally reported in 1968 (equivalent Ca–Ca distances are 3.23 Å, 3.64 Å and 4.35 Å respectively). Additionally, therefore, we observe both thicker N–Ca slabs (2.52 Å *vs.* 2.45 Å) and wider interlayer gaps (3.85 Å *vs.* 3.80 Å) than previously described.[6] The Ca–N bond lengths in both studies are almost within estimated standard deviations and the increased slab thickness stems from elongation of the NCa_6 octahedra parallel to the *c*-axis through *angular* distortion. This angular "stretching" of the NCa_6 octahedra along *c* also accounts for the smaller *a* parameters in our samples of Ca_2N. This type of co-ordination environment is closer to that observed in isostructural Sr_2N than to that seen in the original study of Ca_2N. Interestingly, the ratio of slab thickness (t) to interlayer gap distance (d) calculated from data for Sr_2N[2] is identical to that we observe in Ca_2N ($t/d=0.65$). The origin of the smaller interlayer gap observed by Keve and Skapski is uncertain;[6] the composition of the subnitride in the earlier study was not determined analytically.

The trend in *c*-parameter length and *d* with composition, on the basis of existing data, is a balance of intercalant ionic radius *vs.* $[Ca_2N]^+$ layer repulsion. The nitride hydride, Ca_2NH, forms a cubic NaCl-type superstructure with ordered N^{3-} and H^- anions,[27] yet the equivalent hexagonal *c*-parameter is only 17.53 Å. The implication for the theoretical hexagonally ordered variant is that intercalation of H^- reduces layer repulsion and therefore reduces *d* (and *c*) in accordance with typical Ca–H bond lengths within the gap (with Ca and H at the 6c and 3b sites respectively). The calcium nitride halides, Ca_2NCl ($t/d=2.46/4.11=0.60$) and Ca_2NBr ($t/d=2.43/4.42=0.55$) by contrast show larger *c*-parameters and *d* values than Ca_2N, commensurate with the increasing halide anionic radius and Ca–X bond distances.[28] Ca_2N is intermediate within these extremes with a layer separation increased by repulsion of the positively charged $[Ca_2N]^+$ slabs (or *via* expansion of the electron gas between these layers) relative to theoretical hexagonal Ca_2NH. Addition of larger halides Cl^-, Br^- then forces the layers still further apart. The evidence for the absence of intercalated anions (notably H^-) between layers in our samples of Ca_2N is incontrovertable. Neutron data collected at 298 and 2 K show no fraction of *any* intercalated species present. Furthermore, given the large incoherent scattering cross section of H, the presence of low wt% levels of hydride ions is detectable *via* a characteristic non-linearity in background in the neutron diffraction pattern. None of our data demonstrated this characteristic. Combined with analytical results we are confident that the diffraction data points to the nominal stoichiometry, Ca_2N, being correct.

Bond valence calculations from the POLARIS data at 298 K gave values of 1.3 and 2.6 for Ca and N respectively.[29] These low values are similar to those calculated for alkaline earth metal (A) and N in the strontium subnitride Sr_2N[2] and imply an "incomplete" co-ordination environment for the alkaline earth metal. As in the heavier alkaline earth metal compound, this suggests a formulation based around "$A^{1.5+}$". Alternatively, the compound can be considered to be composed of essentially Ca(II) with free electrons located in the "van der

Table 3 Final atomic parameters for Ca_2N

Data type, Instrument	PXD, Philips Xpert	PND, POLARIS	PND, POLARIS
Sample	I	II	II
Temperature/K	298	298	2
Ca (6c) (0, 0, *z*):			
z	0.2676(1)	0.26756(4)	0.26743(5)
B_{iso}/Å^2	1.42(2)	—	—
$100\times U_{11}=U_{22}$/Å^2	—	0.89(2)	0.06(3)
$100\times U_{33}$/Å^2	—	1.76(6)	1.08(7)
$100\times U_{12}$/Å^2	—	0.45(1)	0.03(1)
N (3a) (0 ,0, 0):			
B_{iso}/Å^2	2.2(1)	—	—
$100\times U_{11}=U_{22}$/Å^2	—	0.55(1)	0.08(2)
$100\times U_{33}$/Å^2	—	1.78(4)	1.39(6)
$100\times U_{12}$/Å^2	—	0.278(8)	0.04(1)

[a]where $B_{iso}=4/3[a^2B_{11}+b^2B_{22}+c^2B_{33}+ab(\cos\gamma)B_{12}+ac(\cos\beta)B_{13}+bc(\cos\alpha)B_{23}]$, $U_{iso}=4/3[a^2U_{11}+b^2U_{22}+c^2U_{33}+ab(\cos\gamma)U_{12}+ac(\cos\beta)U_{13}+bc(\cos\alpha)U_{23}]$ and $B_{iso}=8\Pi^2U_{iso}$.

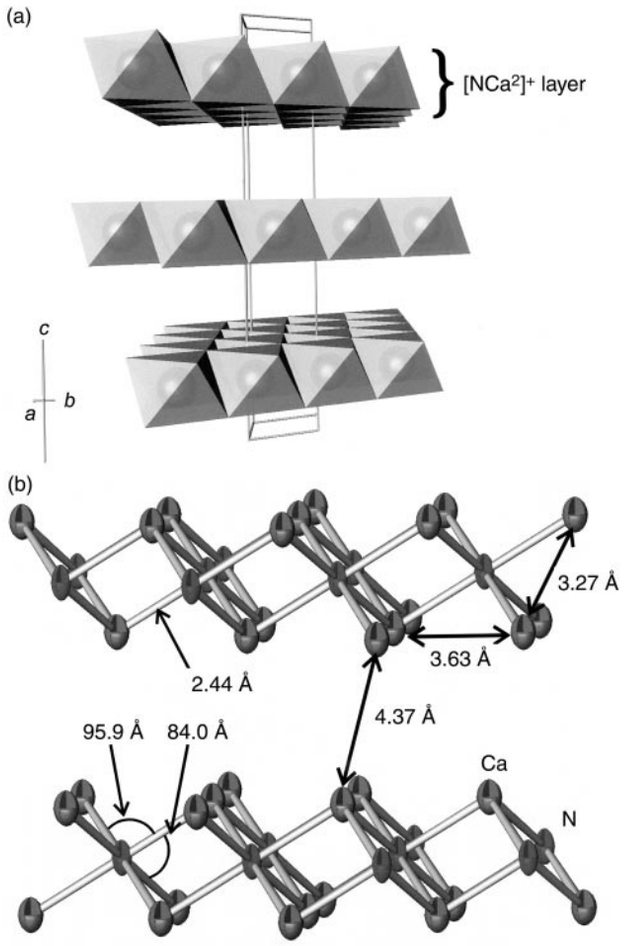

Fig. 4 Structure of Ca_2N: (a) polyhedral, perspective representation showing slabs of edge-sharing NCa_6 octahedra stacked along the crystallographic *c*-axis, (b) ball and stick, ORTEP-style plot of $[NCa_2]^+$ layers showing N and Ca co-ordination, with important distances and angles marked.

Waals gap'' between layers, *i.e.* $Ca^{2+}{}_2N^{3-}\cdot[e^-]$. This latter description is analogous with the bonding seen in 1D (*e.g.* $Na^+{}_nBa^{2+}{}_3N^{3-}\cdot[\{n+3\}e^-]$; $n=0$, 1, 5)[3,10] and 3D (*e.g.* $Ca^{2+}{}_3Au^-\ N^{3-}\cdot[2e^-]$)[14] structural systems and is consistent with the electronic properties observed in Ca_2N and other subnitrides. Also perhaps worth noting is that the valence sum for Ca in the ionic nitride α-Ca_3N_2[4] remains below 2 (1.7).

The relationship between *intra*layer and *inter*layer metal–metal distances in Ca_2N mirrors that in Sr_2N and is analogous to the *intra*- and *inter*chain Ba–Ba distances in the 1D subnitrides, Na_xBa_3N. The insinuation, therefore, is that in each of these alkaline earth (A) subnitrides, the common NA_6 octahedron is an ionic entity and that the large distances between assemblages of these species are brought about by expansion of the surrounding electron gas, as discussed by Steinbrenner and Simon with relation to barium subnitrides.[3]

Table 4 Interatomic distances and angles in Ca_2N

Data	PXD (I)	PND (II)	PND (II)
T/K	298	298	2
N–Ca × 6/Å	2.4403(8)	2.4426(4)	2.4395(4)
Ca–Ca × 3/Å[a]	3.270(1)	3.2706(10)	3.2689(13)
Ca–Ca′ × 6/Å[a]	3.624(1)	3.6287(6)	3.6219(8)
Ca–Ca″ × 3/Å[b]	4.386(2)	4.3742(2)	4.3669(3)
Ca–N–Ca × 6/°	95.88(2)	95.94(1)	95.87(2)
	84.12(4)	84.06(3)	84.14(3)
N–Ca–N × 3/°	95.88(2)	95.94(1)	95.87(2)

[a]Intralayer distance. [b]Interlayer distance.

Electrical conductivities and magnetic susceptibilities of subnitrides and related materials are listed in Table 5. The conductivity we observe for Ca_2N at 293 K is of the same order as that previously observed in Ba_2N. Similarly, metallic conductivity was originally reported in Ca_2N. Despite the higher values reported for Sr_2N (which vary by an order of magnitude), it is clear that the A_2N compounds exhibit conductivities that are comparatively much lower than those of the respective alkaline earth metals themselves (by *ca.* 10^6).[30] The magnitude of the magnetic susceptibility for Ca_2N is in agreement with Sr_2N at room temperature. The previously reported temperature independence of χ_M for A_2N compounds is consistent with weak (Pauli) paramagnetism.

In the light of recent progress in this area, it is of value to briefly contrast the structural and electronic aspects of the A_2N compounds with the only known 1D alkaline earth binary subnitride, Ba_3N, and other ''excess electron'' compounds, Cs_3O (isostructural with Ba_3N) and Ag_2F (with the *anti* CdI_2 structure). Ba_3N, Cs_3O and Ag_2F are better electronic conductors than A_2N compounds by orders of magnitude, with values much closer to those of the respective metals. The expectation is that A_2N compounds exhibit high electrical conductivity in two dimensions—parallel to $[NA_2]^+$ layers—and much poorer conduction in the *c* direction—perpendicular to the layers. The ionic layers can be perceived as barriers to conduction. This hypothesis has yet to be tested on single crystalline samples and inevitably compressed pellets of polycrystalline powders have demonstrated relatively poor conductivity. Ba_3N behaves as a 3D metal like Cs_3O, with conduction electrons free to move between insulating $[A_3X]^{n+}$ cores.

Recent anisotropic electronic measurements on Ag_2F confirm that the subfluoride is truly metallic in three dimensions with no structural barriers to conduction and conductivity of the same order as Ag metal.[30] Band structure calculations also support the premise that Ag_2F is a three dimensional metal.[31] Expansion of ''$[FAg_2]^+$'' layers along *c* relative to $[NA_2]^+$ layers in A_2N compounds and consequent reduction of *d*, give a layer thickness *larger* than the interlayer

Table 5 Electrical conductivities and magnetic susceptibilities for alkaline earth subnitrides and related materials

Compound	Electrical conductivity, σ/Ω^{-1} cm^{-1}[a]	Magnetic susceptibility, χ_m/emu mol^{-1}[a]	Reference
Ca_2N	(i) 1.6×10^{-2}[b]	(i) 2.0×10^{-3}[b]	(i) This work
	(ii) 2.0×10^{-1}		(ii) 6*b*
Sr_2N	(i) 60.0[c]	(i) 1.4×10^{-3}[c]	(i) 2, (ii) 33
	(ii) 5.0	(iii) 2.2×10^{-4}	(iii) 34,
		(iv) 1.5×10^{-4}[b]	(iv) 35
Ba_2N	1.0×10^{-2}	—	36
Ba_3N	8.3×10^{3}[b]	—	3
Ag_2F	(i) 4.0×10^{4}[e]	(ii) -5.8×10^{-5}	(i) 37, (ii) 38
	(ii) $\approx1\times10^{6}$[f], 1.4×10^{5}[e]		(iii) 39
	(iii) 7.7×10^{3}[f], 9.1×10^{4}[e]		
Cs_3O	1.4×10^{4}[d]	6.1×10^{-5}[d]	40

[a]Measured at 298 K unless stated otherwise. [b]At 293 K. [c]At 300 K. [d]At 303 K. [e]σ parallel to layers. [f]σ perpendicular to layers.

gap distance and $t/d = 1.57$. Crucially, Ag–Ag distances *between* layers (2.81 Å) are not larger than those *within* layers (3.00 Å) and both distances are comparable to those in Ag metal (2.89 Å).[32]

In summary, we have described in detail a systematic study of synthetic routes to dicalcium nitride, Ca_2N, and thoroughly investigated composition, structural chemistry and crystallite morphology. Measurements on microcrystalline samples indicate metallic conductivity and paramagnetic behaviour at room temperature. We have now also synthesised single crystals of subnitrides, but need to optimise our synthesis routes to produce crystals of sufficient size for extensive structure and anisotropic property investigations. Such future studies of bulk and crystalline materials will illuminate further the conduction processes in "excess electron" compounds and the nature of the bonding within these materials.

Acknowledgements

The authors thank Dr R. I. Smith for his extensive help in collecting the POLARIS data and Dr M. G. Barker for use of equipment in this work. D.H.G. acknowledges the EPSRC for the award of an Advanced Fellowship and for financial support of this work under grant GR/M20921. We also thank the Nuffield Foundation for the award of an Undergraduate Bursary (NUF-URB98) to A. B and the CLRC for award of direct access beam time.

References

1 See for example A. Rabenau and H. Schulz, *J. Less-Common Met.*, 1976, **50**, 155.
2 N. E. Brese and M. O'Keeffe, *J. Solid State Chem.*, 1990, **87**, 134.
3 U. Steinbrenner and A. Simon, *Z. Anorg. Allg.Chem.*, 1998, **624**, 228.
4 Y. Laurent, J. Lang and M. Th. Le Bihan, *Acta Crystallogr., Sect. B*, 1968, **24**, 494.
5 I. Ahmad, PhD Thesis, London, 1963.
6 (*a*) E. T. Keve and C. Skapski, *Chem. Commun.*, 1966, 829; (*b*) E. T. Keve and C. Skapski, *Inorg. Chem.*, 1968, **7**, 1757.
7 O. Reckeweg and F. J. DiSalvo, *Angew. Chem., Int. Ed.*, 2000, **39**, 412.
8 (*a*) See for example N. E. Brese, M. O'Keeffe and R. B. Von Dreele, *J. Solid State Chem.*, 1990, **88**, 571; (*b*) B. Wegner, R. Essman, J. Bock, H. Jacobs and H. P. Fischer, *Eur. J. Solid State Inorg. Chem.*, 1992, **29**, 1217; (*c*) Th. Sichla, F. Altorfer, D. Hohlwein, K. Reimann, M. Steube, J. Wrzesinski and H. Jacobs, *Z. Anorg. Allg. Chem.*, 1997, **623**, 414.
9 See for example C. Röhr, *Angew. Chem., Int. Ed. Engl.*, 1996, **35**, 1199 and references therein..
10 (*a*) P. E. Rauch and A. Simon, *Angew. Chem., Int. Ed. Engl.*, 1992, **31**, 1519; (*b*) G. J. Snyder and A. Simon, *J. Am. Chem. Soc.*, 1995, **117**, 1996.
11 G. J. Snyder and A. Simon, *Angew. Chem., Int. Ed. Engl.*, 1994, **33**, 689.
12 O. Reckweg, T. P. Braun, F. J. DiSalvo and H.-J. Meyer, *Z. Anorg. Allg. Chem.*, 2000, **626**, 62.
13 P. F. Henry and M. T. Weller, *Angew. Chem., Int. Ed.*, 1998, **37**, 2855.
14 J. Jäger, D. Stahl, P. C. Schmidt and R. Kniep, *Angew. Chem., Int. Ed. Engl.*, 1993, **32**, 709.
15 D. H. Gregory, M. G. Barker, P. P. Edwards and D. J. Siddons, *Inorg. Chem.*, 1995, **34**, 5195.
16 Y. Laurent, J. Lang and M. Th. Le Bihan, *Acta Crystallogr., Sect. B*, 1968, **24**, 494.
17 M. G. Barker, M. J. Begley, P. P. Edwards, D. H. Gregory and S. E. Smith, *J. Chem. Soc., Dalton Trans.*, 1996, 1.
18 D. Louer and M. Louer, *J. Appl. Crystallogr.*, 1972, **5**, 271.
19 A. Boultif and D. Louer, *J. Appl. Crystallogr.*, 1991, **24**, 987.
20 G. Nolze and W. Kraus, *Powder Diffract.*, 1998, **13**, 256.
21 H. M. Rietveld, *J. Appl. Crystallogr.*, 1969, **2**, 65.
22 (*a*) D. B. Wiles and R. A. Young, *J. Appl. Crystallogr.*, 1981, **14**, 149; (*b*) C. J. Howard and R. J. Hill, Report No. M112: Australian Atomic Energy Commission, Menai, Australia, 1986.
23 J. Rodriguez-Carvajal, *Physica B*, 1993, **192**, 55.
24 A. Larson and R. B. von Dreele, The General Structure Analysis System, Los Alamos National Laboratory, 1985.
25 W. H. Baur, *Crystallogr. Rev.*, 1987, **1**, 59.
26 W. B. Pearson, *The Crystal Chemistry and Physics of Metals and Alloys*, Wiley-Interscience, New York, 1972.
27 (*a*) J.-F. Brice, J.-P, Motte, A. Courtois, J. Protas and J. Aubry, *J. Solid State Chem.*, 1976, **17**, 135; (*b*) T. Sichla and H. Jacobs, *Eur. J. Solid State Inorg. Chem.*, 1995, **32**, 49.
28 C. Hadenfeldt and H. Herdejürgen, *Z. Anorg. Allg. Chem.*, 1987, **545**, 177.
29 N. E. Brese and M. O'Keeffe, *Acta Crystallogr., Sect. B*, 1991, **47**, 192.
30 G. T. Meaden, *Electrical Resistance of Metals*, Heywood, London, 1966.
31 N. Hamada, S. Ido, K. Kitazawa and S. Tanaka, *J. Phys.C: Solid State Phys.*, 1986, **19**, 1355.
32 (*a*) G. Argay and I. Naray-Szabo, *Acta Chim. Acad. Sci. Hung.*, 1966, **49**, 329; (*b*) A. Williams, *J. Phys.: Condens. Matter*, 1989, **1**, 2569.
33 J. Gaudé, P. L'Haridon, Y. Laurent and J. Lang, *Bull. Soc. Fr. Miner. Cristallogr.*, 1972, **95**, 56.
34 J. Gaudé, P. L'Haridon, Y. Laurent and J. Lang, *Rev. Chim. Miner.*, 1971, **8**, 287.
35 S. M. Ariya, M. S. Erofeeva and G. P. Machaloy, *J. Gen. Chem. USSR*, 1957, **27**, 1806.
36 S. M. Ariya, E. A. Prokofyeva and I. I. Matveeva, *J. Gen. Chem. USSR*, 1955, **25**, 609.
37 R. Hilsch, G. V. Minnigerode and H. V. Wartenberg, *Naturwiss.*, 1957, **44**, 463.
38 S. Ido, S. Uchida, K. Kitazawa and S. Tanaka, *J. Phys. Soc. Jpn.*, 1988, **57**, 997.
39 X. Wang and I. Ikezawa, *J. Phys. Soc. Jpn.*, 1991, **60**, 1398.
40 K.-R Tsai, P. M. Harris and E. N. Lassettre, *J. Phys. Chem.*, 1956, **60**, 345.